Arctic Sea Ice in CMIP6

Dirk Notz, Jakob Dörr, David H. Bailey, Ed Blockley, Mitchell Bushuk, Jens Boldingh Debernard, Evelien Dekker, Patricia Derepentigny, David Docquier, Neven Fučkar, et al.

Geophysical Research Letters

RESEARCH LETTER
10.1029/2019GL086749

Key Points:
- CMIP6 model simulations of Arctic sea-ice area capture the observational record in the multimodel ensemble spread
- The sensitivity of Arctic sea ice to changes in the forcing is better captured by CMIP6 models than by CMIP5 and CMIP3 models
- The majority of available CMIP6 simulations lose most September sea ice for the first time before 2050 in all scenarios

Supporting Information:
- Supporting Information S1

Correspondence to:
D. Notz,
dirk.notz@mpimet.mpg.de

Citation:
SIMIP Community (2020). Arctic sea ice in CMIP6. *Geophysical Research Letters*, *47*, e2019GL086749. https://doi.org/10.1029/2019GL086749

Received 22 DEC 2019
Accepted 12 APR 2020
Accepted article online 17 APR 2020

Arctic Sea Ice in CMIP6

SIMIP Community

Abstract We examine CMIP6 simulations of Arctic sea-ice area and volume. We find that CMIP6 models produce a wide spread of mean Arctic sea-ice area, capturing the observational estimate within the multimodel ensemble spread. The CMIP6 multimodel ensemble mean provides a more realistic estimate of the sensitivity of September Arctic sea-ice area to a given amount of anthropogenic CO_2 emissions and to a given amount of global warming, compared with earlier CMIP experiments. Still, most CMIP6 models fail to simulate at the same time a plausible evolution of sea-ice area and of global mean surface temperature. In the vast majority of the available CMIP6 simulations, the Arctic Ocean becomes practically sea-ice free (sea-ice area $<1 \times 10^6$ km^2) in September for the first time before the Year 2050 in each of the four emission scenarios SSP1-1.9, SSP1-2.6, SSP2-4.5, and SSP5-8.5 examined here.

Plain Language Summary We examine simulations of Arctic sea ice from the latest generation of global climate models. We find that the observed evolution of Arctic sea-ice area lies within the spread of model simulations. In particular, the latest generation of models performs better than models from previous generations at simulating the sea-ice loss for a given amount of CO_2 emissions and for a given amount of global warming. In most simulations, the Arctic Ocean becomes practically sea-ice free (sea-ice area <1 million km^2) in September for the first time before the Year 2050.

1. Introduction

In recent decades, Arctic sea-ice area has decreased rapidly, and the signal of a forced sea ice retreat has clearly emerged from the background noise of year-to-year variability. Because of this, the ability of climate models to plausibly simulate the observed changes in Arctic sea-ice coverage has become a central measure of model performance in Arctic-focused climate-model intercomparisons (e.g., Koenigk et al., 2014; Massonnet et al., 2012; Melia et al., 2015; Olonscheck & Notz, 2017; Shu et al., 2015; Stroeve et al., 2007, 2012, 2014). In this contribution, we extend these earlier studies that examined model performance in the third and fifth phases of the Coupled Model Intercomparison Project (CMIP3 and CMIP5) by examining model simulations from the sixth phase of the Coupled Model Intercomparison Project (CMIP6, Eyring et al., 2015). For CMIP6, the Sea-Ice Model Intercomparison Project (SIMIP Notz et al., 2016) designed a specific set of diagnostics that allow for detailed analyses of sea ice related processes and thus a process-based evaluation of sea ice simulations of the participating models. To lay the foundation for such analyses, we here provide an initial overview of CMIP6 model performance by examining some large-scale, pan-Arctic metrics of model performance and future sea-ice evolution, including a comparison to CMIP5 and CMIP3 simulations. A similar analysis for Antarctic sea ice is given by Roach et al. (2020).

2. Analysis Method

In this contribution, we examine two large-scale integrated quantities that describe the time evolution of Arctic sea ice. These are the Northern Hemisphere total sea-ice area and total sea-ice volume, which can be calculated readily from SIMIP variables as follows.

To obtain sea-ice area for CMIP6 model simulations, we use the SIMIP variable of Northern Hemisphere sea-ice area `siarean` when provided. If `siarean` is not provided, we calculate the sea-ice area by multiplying sea-ice concentration on the ocean grid (`siconc`, preferred) or on the atmospheric grid (`siconca`) with individual grid-cell area and then sum over the Northern Hemisphere. Note that we use sea-ice area as our primary variable to describe sea-ice coverage instead of sea-ice extent, which is usually calculated as the total area of all grid cells with at least 15% sea-ice concentration. Our choice to focus on sea-ice area derives primarily from the fact that sea-ice extent is a strongly grid-dependent, nonlinear quantity, making it difficult to meaningfully compare between model output and satellite observations (cf. Notz, 2014). In addition,

the observational spread across different satellite products is smaller for trends in sea-ice area than it is for trends in sea-ice extent (Comiso et al., 2017).

To calculate sea-ice volume for CMIP6 models, we (1) directly use the SIMIP variable of Northern Hemisphere sea-ice volume `sivoln` when provided, or (2) multiply the sea-ice volume per grid-cell area `sivol` by individual grid-cell area and sum over the Northern Hemisphere, or (3) multiply sea-ice concentration `siconc`, sea-ice thickness `sithick`, and individual grid-cell area and then sum over the Northern Hemisphere. For CMIP5, only the sea-ice volume per grid-cell area (also called "equivalent sea-ice thickness," `sit`) is available, so we use method (2) for all CMIP5 models. We were unable to obtain sea-ice volume data for CMIP3 models, so volume comparisons in the following are limited to CMIP5 and CMIP6 model simulations.

To meaningfully estimate model performance relative to the real evolution of the sea-ice cover in the Arctic, we must take internal variability into account (see, e.g., England et al., 2019; Kay et al., 2011; Notz, 2015; Olonscheck & Notz, 2017; Swart et al., 2015). Internal variability describes the spread in plausible climate trajectories in response to a given forcing scenario, owing to the chaotic nature of our climate system. The observational record is just one such plausible trajectory, and no single model simulation can ever be expected to perfectly agree with it because of its chaotic nature. Therefore, most CMIP6 models have been run several times with slightly different initial conditions to estimate the range of trajectories that are compatible with a given model's physics. In the following, we take two different approaches to examine whether a given model provides a plausible simulation of the observational record in light of internal variability.

First, for CMIP6 models, we estimate a best-guess CMIP6-average internal variability σ_{cmip6} by averaging across the individual ensemble spread of those models that provide three or more ensemble members (see Table S3 in the supporting information for details). In calculating the standard deviation, we correct for small sample size n by using Bessel's correction and then dividing the resulting standard deviation by the scale mean of the chi distribution with $n-1$ degrees of freedom. We then define all simulations that lie within the range of $2\sigma = \pm 2\sqrt{\sigma_{cmip6}^2 + \sigma_{obs}^2}$ around the observational estimate as plausible simulations (cf. Olonscheck & Notz, 2017). Here, σ_{obs}^2 refers to the observational uncertainty explained below. This approach allows us to also examine the plausibility of those models that only provide a single ensemble member. In addition to considering internal variability explicitly, we reduce its impact by examining model performance relative to a time average over several years. We take the first 20 years of the satellite record (1979–1998) for comparing mean values, as those 20 years provide a compromise between using as many years as possible and using a period with no strong trend in Arctic sea-ice area and volume. However, even on multidecadal time scales internal variability affects the Arctic sea-ice cover, so averaging over 20 years is not long enough an averaging period to remove the impact of internal variability entirely. To compare trends, we examine the overlap period 1979–2014 of the satellite record, which begins in 1979, and the historical period of CMIP6, which ends in 2014.

Second, in order to select a subset of models for estimating a best guess of the future evolution of the Arctic sea-ice cover, we take the more strict approach to define a model as plausible if its ensemble spread includes the observational record, considering observational uncertainty. These models are referred to as "selected models" hereafter.

To obtain an observational estimate of sea-ice area, we use observational records of sea-ice concentration from the OSI SAF (Lavergne et al., 2019), NASA-Team (Cavalieri et al., 1997) and Bootstrap (Comiso et al., 1997) algorithms. sea-ice area is then calculated by multiplying the sea-ice concentration with individual grid-cell area and summing over the Northern Hemisphere. For the NASA-Team and Bootstrap algorithms, we filled the observational pole hole with the average sea-ice concentration around its edge (Olason & Notz, 2014). For OSI SAF, we used the filled pole hole of the product itself. We take the spread of the three algorithms obtained this way as the observational uncertainty σ_{obs}.

For sea-ice volume, we do not compare models with an observational estimate due to substantial uncertainties for reanalysed and observed estimates of Arctic sea-ice thickness and thus volume (e.g., Bunzel et al., 2018; Chevallier et al., 2017; Zygmuntowska et al., 2014).

For global mean surface temperature (GMST), we use the average of NOAAGlobalTemp v5.0.0 (Vose et al., 2012), GISTemp v4 (GISTEMP Team, 2019; Lenssen et al., 2019), HadCRUT4.6.0.0 (Morice et al., 2012), and Berkeley (Rohde et al., 2013) time series as an estimate for the mean evolution and the spread across

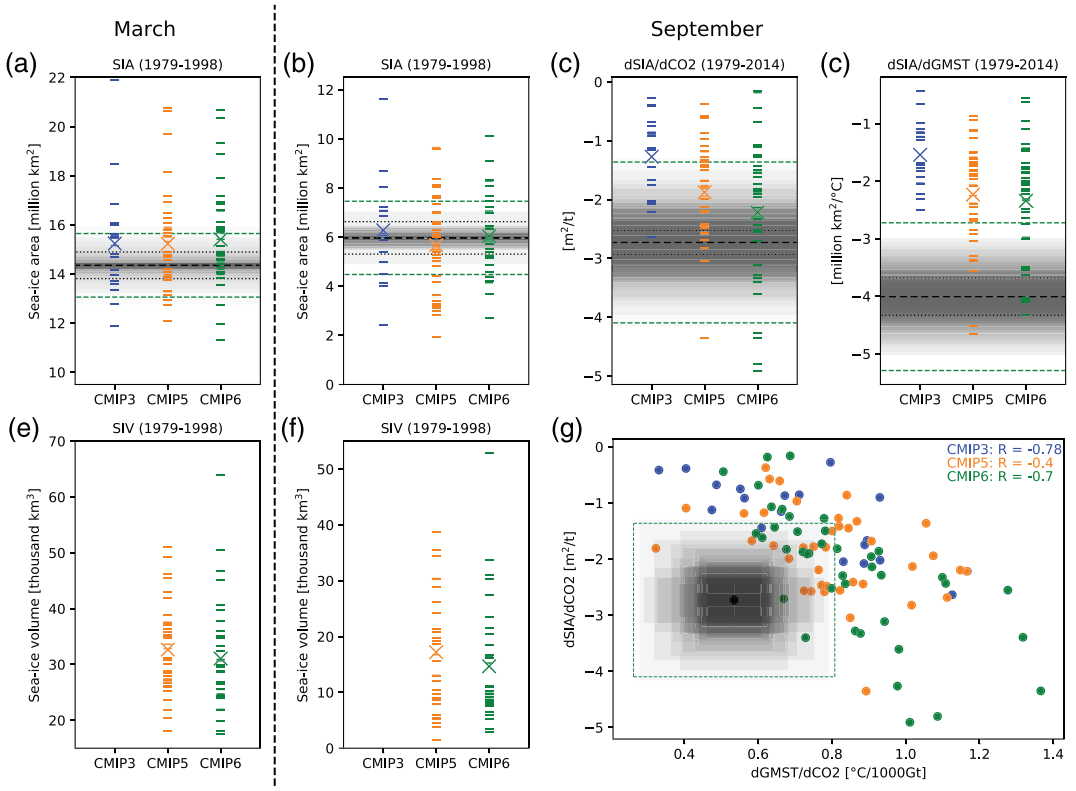

Figure 1. Comparison of sea ice metrics as simulated by the first ensemble members of CMIP3 (blue), CMIP5 (orange), and CMIP6 (green) models. The individual panels show the mean Arctic sea-ice area (SIA) in (a) March and (b) September for 1979–1998; mean Arctic sea-ice volume (SIV) in (e) March and (f) September for 1979–1998; and (c, d) the sensitivity over the period 1979–2014 of September sea-ice area to (c) CO_2 emissions and (d) global annual mean surface temperature (GMST). (g) The sensitivity of Arctic sea-ice area to CO_2 emissions scattered against the sensitivity of GMST to CO_2 emissions. In (a)–(f), horizontal dashes represent the first ensemble member of each model and crosses represent the multimodel ensemble mean. The thick dashed black lines denote the average of the observational satellite products, where available. The dotted lines denote one standard deviation of observational uncertainty. The green dashed lines denote the 2σ plausible range including internal variability and observational uncertainty as defined in section 2. The gray shadings around the lines denote overlays of estimated internal variability from all CMIP6 models with three or more ensemble members, with each overlay representing the 1 standard deviation spread of a single model. Hence, the darker the shading, the more models agree on internal variability to cover a certain range.

these four records as an estimate for observational uncertainty. We calculate anomalies relative to the period 1850–1900, except for the shorter record of NOAAGlobalTemp where we calculate anomalies relative to 1880–1900. Because the 20-year running mean temperature fluctuations during these periods are less than 0.1°C, our results are largely insensitive to this choice of baseline period (Figure S2). We take the spread of the four products as the observational uncertainty σ_{obs}.

Historical anthropogenic CO_2 emissions are taken from the historical budget of the Global Carbon Project (Global Carbon Project, 2019). Future anthropogenic CO_2 emissions for CMIP6 simulations are taken from the respective SSP scenarios described by Riahi et al. (2017).

3. CMIP6 Model Performance

3.1. Mean Quantities

We start with an analysis of the mean sea-ice fields simulated by individual CMIP3, CMIP5, and CMIP6 models (Figures 1a, 1b, 1e, and 1f) over the period 1979–1998. To allow for a fair comparison across the three CMIP phases, in this section we analyze only the first ensemble member of each model. Given the large number of participating models, this results in a fair comparison: For models with several ensemble members, the first ensemble member is as likely to be above a model's ensemble mean as below.

For sea-ice area, we find a large spread across CMIP6 simulations both in March and in September (Figures 1a and 1b), which usually are the months of maximum and minimum sea-ice coverage in the Arctic, respectively. In March, the 1979–1998 mean sea-ice area simulated by CMIP6 models ranges from around 12×10^6 km^2 to more than 20×10^6 km^2 and thus includes the observational estimate of 14.4×10^6 km^2 (Figure 1a and Table S3). Out of the 40 CMIP6 models, 21 are within the $2\sigma = \pm 1.29 \times 10^6$ km^2 plausibility range around the observational estimate given by the CMIP6-average internal variability and observational uncertainty as introduced in section 2 (Figure 1a and Table S3). CMIP3 and CMIP5 simulations also show a large spread in mean March sea-ice area and include the observational estimate within their multimodel ensemble spread (Figure 1a and Tables S1 and S2). However, in CMIP3 and CMIP5, the multimodel ensemble spread is more evenly distributed around the observational estimate than in CMIP6, where most models lie above it.

For the mean September sea-ice area over the period 1979–1998, the CMIP6 ensemble also shows a large spread of individual simulations, ranging from around 3×10^6 km^2 to around 10×10^6 km^2 (Figure 1b and Table S3). The observed value of around 6×10^6 km^2 lies well within the range, and 25 out of 40 CMIP6 models are within the plausible range of $2\sigma = \pm 1.49 \times 10^6$ km^2 around this value (Table S3). The CMIP6 multimodel ensemble mean is very close to the observational estimate and well within the plausible range. The same holds for CMIP3 and CMIP5, with their individual models also spanning a wide range around the observational estimate (Figure 1b and Tables S1 and S2).

For sea-ice volume, we lack data for CMIP3 models and thus can only compare CMIP6 results to CMIP5 results (see Tables S2 and S3 for a detailed overview). For both phases of CMIP, the models produce a similar spread of simulated Arctic sea-ice volume from less than 20,000 km^3 to more than 40,000 km^3 in March (Figure 1e), and from less than 5,000 km^3 to more than 30,000 km^3 in September (Figure 1f). Given a simulated average spread from internal variability of around 2,000 km^3, the large spread in sea-ice volume from CMIP6 models can not be explained by internal variability alone. Instead, it is caused by the models' large spread in simulated sea-ice area and thickness.

Based on this analysis of mean Arctic sea ice quantities, we find that there is little difference in overall model performance between CMIP3, CMIP5 and CMIP6. The multimodel spread of the mean quantities remains large, the observational record lies within the multimodel ensemble spread, and many models simulate plausible values of mean sea-ice area when considering the impact of internal variability and observational uncertainty. The multimodel ensemble means of the past three phases of CMIP are relatively similar to each other and largely consistent with the observational record.

3.2. Sensitivity

In addition to their plausible simulation of mean quantities, the models' adequacy for simulating reality hinges critically on their ability to realistically simulate the response of a given climate metric to changes in external forcing. Internal variability causes a large spread of plausible climate trajectories in response to a given change in the forcing and must carefully be taken into account when interpreting a possible mismatch between a simulation and a given observational sea ice record (Jahn et al., 2016; Kay et al., 2011; Notz, 2015; Olonscheck & Notz, 2017; Swart et al., 2015). We find this to remain valid for CMIP6 simulations.

For our analysis of the simulated sensitivity of Arctic sea ice to changes in external forcing, we calculate two distinct quantities: first, the change in sea-ice area for a given change in cumulative anthropogenic CO_2 emissions over the period 1979–2014 (Figure 1c) and second, the change in sea-ice area for a given change in GMST over the period 1979–2014 (Figure 1d). Both quantities can be calculated from the previously demonstrated linear relationships of sea-ice area to cumulative CO_2 emissions (Herrington & Zickfeld, 2014; Notz & Stroeve, 2016; Zickfeld et al., 2012) and to GMST (e.g., Gregory et al., 2002; Mahlstein & Knutti, 2012; Rosenblum & Eisenman, 2016; Stroeve & Notz, 2015; Winton, 2011). Together, these two quantities allow us to estimate whether CMIP6 models simulate changes in sea ice with the correct sensitivity to changes in external forcing and whether they potentially do so for the right reason. This is because the relationship between sea-ice area and cumulative anthropogenic CO_2 emissions is an almost linear proxy for the long-term time evolution of Arctic sea-ice area, as cumulative emissions map monotonously to time. In contrast, the sensitivity of sea-ice area to GMST changes is a proxy for the sensitivity of the sea-ice cover to one particular response of the climate system to changes in external forcing.

Our analysis reveals that over the historical period 1979–2014, 28 out of 40 CMIP6 models simulate a sensitivity of the Arctic sea-ice area to cumulative anthropogenic CO_2 emissions that is within the plausible range of 2.73 ± 1.37 m^2 of sea-ice loss per ton of CO_2 emissions (Figure 1c and Table S3). In addition to the larger spread of the CMIP6 multimodel ensemble, a major difference between CMIP5 and CMIP6 models is that, in their first ensemble member analyzed here, only 3 out of 40 CMIP5 models simulate a larger loss of sea-ice area per ton of CO_2 emissions than observed. This number increases to 10 out of 40 models for CMIP6. This results in the CMIP6 multimodel ensemble mean being closer to the observational estimate than the CMIP5 and the CMIP3 multimodel ensemble means. It is, however, unclear whether this reflects an improvement of model physics or primarily arises from the change in historical forcing in CMIP6 relative to CMIP5 (cf. Rosenblum & Eisenman, 2016). For example, in CMIP6 the historical ozone radiative forcing is about 80 % higher than it was in CMIP5 (Checa-Garcia et al., 2018). In contrast, black carbon emissions in the CMIP6 historical forcing are substantially higher over the past years than prescribed in the CMIP5 RCP8.5 scenario (Gidden et al., 2019). The impact of these changes in non-CO_2 climate drivers is confounded into the sensitivity of sea-ice area to CO_2 emissions (again, cf. Rosenblum & Eisenman, 2016). Emissions of CO_2 itself, and of methane, are largely unchanged over the historical period for CMIP5 and CMIP6. However, for the future simulations the CMIP6 SSP5-8.5 scenario assumes higher CO_2 emissions and lower methane emissions than the CMIP5 RCP8.5 scenario (Gidden et al., 2019).

Examining the sea-ice loss per degree of global warming, we find that only 11 out of 40 CMIP6 models are within the plausible range of $4.01 \pm 1.28 \times 10^6$ m^2 of sea-ice loss per degree of warming (Figure 1d and Table S3). This is comparable to CMIP5, where 9 out of 40 models were within this plausible range (Figure 1d and Table S2). In CMIP3, not a single model provided a plausible sensitivity (Figure 1d). Also, the CMIP6 multimodel ensemble mean of Arctic sea-ice loss for a given amount of global warming is closer to (but still outside) the plausible range than the multimodel ensemble mean of both CMIP5 and CMIP3. This might indicate an improvement of CMIP6 models over previous CMIP phases on a process level, given that the main physical link of sea-ice loss to any change in external forcing is given by a change in temperature. However, as before, this might also be a reflection of a more realistic historical forcing of CMIP6 compared to CMIP5 and CMIP3.

While the more realistic simulation of these two sensitivities might indicate progress in CMIP6 models' capability to simulate the ongoing loss of Arctic sea ice, as in CMIP5 (Rosenblum & Eisenman, 2017) few CMIP6 models are able to simulate a plausible amount of sea-ice loss and simultaneously a plausible change in global mean temperature over time (or cumulative anthropogenic CO_2 emissions). Of the CMIP6 models analyzed here, these are ACCESS-CM2, BCC-CSM2-MR, CNRM-CM6-1-HR, FGOALS-f3-L, FIO-ESM-2-0, GFDL-ESM4, GISS-E2-1-G, GISS-E2-1-G-CC, MPI-ESM-1-2-HAM, MPI-ESM1-2-HR, MPI-ESM1-2-LR, MRI-ESM2-0, and NorESM2-MM. For the other CMIP6 models, those models that have a reasonable sea-ice loss tend to have too much global warming, while those models that simulate reasonable global warming simulate too little sea-ice loss (Figure 1g and Table S3). In particular, the models with a high sensitivity of Arctic sea-ice area to anthropogenic CO_2 emissions also display a high sensitivity of global mean temperature to CO_2 emissions. Hence, understanding this high climate sensitivity is most likely key to understanding why some CMIP6 models display such rapid loss of Arctic sea ice. A recent study suggested this high sensitivity to be caused by stronger cloud feedbacks (Zelinka et al., 2020).

If we plot the two sensitivity metrics against each other, it is generally impossible to distinguish a given CMIP6 model from the cloud given by CMIP5 models, with the exception of the highly sensitive CMIP6 simulations that clearly fall outside the cloud of previous CMIP phases (Figure 1g). The lack of both such high-sensitive simulations and of very low-sensitive simulations in CMIP5 might be one reason that the correlation between the two metrics is lower for CMIP5 than for CMIP3 and CMIP6.

In summary, we find that over the period 1979–2014, CMIP6 models on average simulate a sensitivity of Arctic sea ice that is closer to the observed value than CMIP5 and CMIP3 models, both relative to a given CO_2 emission (as a proxy for time) and to a given warming. However, only few models are able to simulate a plausible sea-ice loss sensitivity to cumulative CO_2 emissions and simultaneously a plausible rise in GMST.

4. Projections of Future Arctic Sea Ice

The identified spread of CMIP models in simulating the past mean state and sensitivity to warming and CO_2 emissions introduces significant model uncertainty into future projections of the evolution of the Arctic sea-ice cover. This model uncertainty remains large in CMIP6.

To address this issue when analyzing projections of when Arctic sea-ice area might drop below 1×10^6 km^2, a commonly used threshold for an ice-free Arctic, we take the following approach. First, we examine the full range of CMIP6 model simulations, noting that the model spread provides a wide spectrum of the possible future evolution of Arctic sea-ice area. Second, we narrow the range by considering only those models that have the observations within their ensemble spread simultaneously for two key metrics (cf. Massonnet et al., 2012): (a) the 2005–2014 September mean sea-ice area and (b) the observed sensitivity of sea-ice area to cumulative CO_2 emissions over the period 1979–2014. We choose these metrics because they correlate with the first sea ice-free year at a correlation of $R > 0.5$ for all scenarios over the entire CMIP6 multimodel ensemble. Note, however, that care must be taken when interpreting the range of selected models, as the relationship between past and future evolution of a climate model is not always clear (Jahn et al., 2016; Stroeve & Notz, 2015). On the other hand, it becomes more important that a model plausibly captures the observed mean state of Arctic sea-ice area the lower that mean state becomes, because initial conditions become more important as the observed sea ice state approaches ice-free conditions and the simulations start entering the realm of decadal predictions. We hence trust that the range of uncertainty given by the selected models gives a more realistic estimate of the true model uncertainty than that given by the full CMIP6 multimodel ensemble. The selected models are printed in bold in Table S4.

In analyzing the future relationship between sea-ice loss and changes in the forcing, we find that the simulated correlation between winter Arctic sea-ice area and cumulative CO_2 emissions remains high well into the future (Figure 2a). For summer, the linear relationship eventually decreases as more and more years of zero Arctic sea-ice coverage are averaged into the multimodel mean (Figure 2d). In interpreting these results quantitatively, it is of course important to note that CO_2, while being the most important external driver of observed changes in Arctic sea-ice coverage, is not the only cause of observed and future changes. Its dominant role, however, holds well into the future and/or the additional impacts of other anthropogenic forcings, such as methane and aerosols, remain roughly stable over time. Otherwise, the correlation between March Arctic sea-ice area and cumulative CO_2 emissions would not remain as stable over time and would not be as independent of the specific forcing scenario (Figure 2a).

We also find that the simulated correlation of temperature with winter Arctic sea-ice area remains high well into the future (Figure 2b), while again in summer the correlation eventually decreases as more models lose their sea ice completely (Figure 2e).

The high correlation between sea-ice loss and changes in the forcing allows us to estimate the cumulative future CO_2 emissions, warming level, and eventually year at which the Arctic Ocean will practically be sea-ice free for the first time, defined as the first year in which the monthly mean September sea-ice area drops below 1×10^6 km^2.

We find that CMIP6 models simulate a large spread of cumulative future CO_2 emissions at which the Arctic could first become practically sea-ice free in September (Figure 3a). The simulated future emissions for the first occurrence of a practically sea-ice free Arctic Ocean range from 450 Gt CO_2 *below* to more than 5,000 Gt CO_2 above present cumulative emissions. However, 158 out of 243 simulations become practically sea-ice free before future cumulative CO_2 emissions reach 1,000 Gt CO_2 above that of 2019 (equivalent to about 3,400 Gt CO_2 cumulative emissions since 1850). Considering only the models with ensemble members within the plausible range of observed sea-ice evolution, we find a reduced range of 170 Gt below to 2,200 Gt above cumulative future anthropogenic CO_2 emissions when Arctic sea-ice area is projected to drop below 1×10^6 km^2. Of these members from the selected models, the vast majority (101 out of 128) become practically sea-ice free at future cumulative CO_2 emissions less than 1,000 Gt. This compares favourably with the range of 800 ± 300 Gt estimated from a direct analysis of the observed sensitivity (Notz & Stroeve, 2018). In combination, these estimates make it appear likely that the Arctic Ocean will practically lose its sea-ice cover in September for the first time at future anthropogenic CO_2 emissions of between 200 and 1,100 Gt above that of 2019.

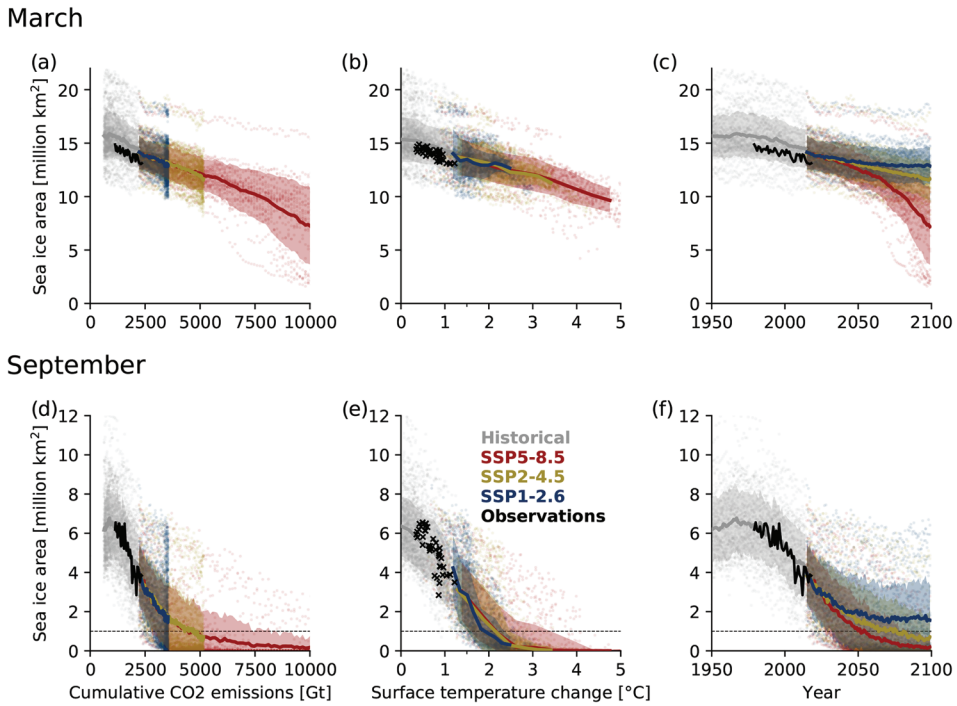

Figure 2. Evolution of Arctic sea-ice area over the historical period and following three scenario projections in (a–c) March and (d–f) September as a function of (a,d) cumulative anthropogenic CO_2 emissions, (b, e) global annual mean surface temperature anomaly, and (c, f) time for all available CMIP6 models. Thick lines denote the multimodel ensemble mean, where all models are represented by their first ensemble member, and the shading around the lines indicates one? standard deviation around the multimodel mean. Faint dots denote the first ensemble member of each model, and thick black lines and crosses denote observations. Note that discontinuities in the multimodel ensemble mean arise from a different number of available models for the historical period and the scenario simulations.

As a function of GMST, ice-free conditions occur across the entire CMIP6 multimodel ensemble at a global warming of between 0.9 and 3.2°C above preindustrial conditions of each individual model (Figure 3b). If we select only those models with a reasonable simulation of past Arctic sea ice conditions, the estimated temperature range decreases slightly to 1.3°C to 2.9°C. The upper end of this range is higher than the range of 1.7 ± 0.4°C estimated from a direct analysis of the observed sensitivity (Notz & Stroeve, 2018) and higher than estimates from bias-corrected simulations that all project the first ice-free Arctic at temperatures below 2°C (Jahn, 2018; Niederdrenk & Notz, 2018; Ridley & Blockley, 2018; Screen & Williamson, 2017; Sigmond et al., 2018). This high bias is probably a reflection of the CMIP6 models' weak sensitivity of sea-ice area loss

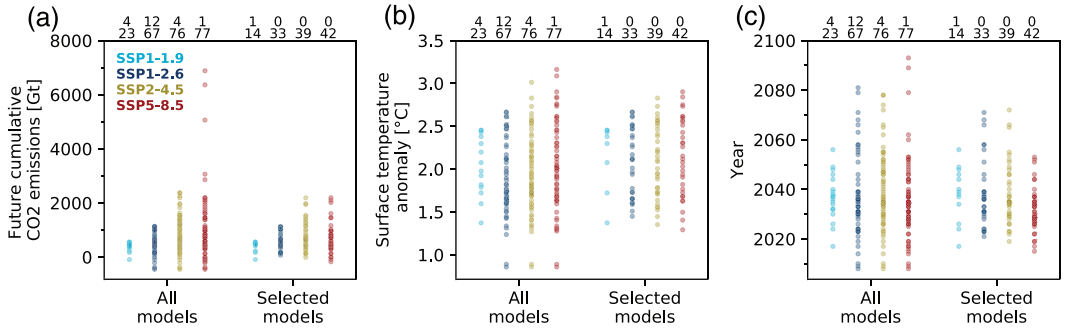

Figure 3. CMIP6 projections of (a) future cumulative CO_2 emissions, (b) global annual mean surface temperature anomaly, and (c) year when September mean sea-ice area drops below 1×10^6 km^2 for the first time in each simulation. The numbers at the top of the panels denote the number of simulations that do not simulate a sea-ice cover below 1×10^6 km^2 by 2100 (top row) and the total number of simulations (bottom row) for each scenario. Each dot represents a single simulation, with all available CMIP6 simulations shown in the figure.

to global warming, resulting in too high estimates of the warming at which the Arctic becomes practically sea-ice free in summer.

In the CMIP6 ensemble, the sea-ice area loss per cumulative CO_2 emissions and degree of global warming does barely depend on the forcing scenario (Figures 3a and 3b). Scenario dependence is also very small regarding the near-term future evolution of Arctic summer sea ice as a function of time until about 2040 (Figures 2f and 3c). This is related to the fact that until 2040, the scenarios evolve quite similarly (O'Neill et al., 2016). Furthermore, given that the current sea-ice area is much smaller than it used to be, the importance of internal variability increases relative to the forced change necessary to lose the remaining sea-ice cover in September. As a consequence, for some models the sea ice disappears earlier for the low-emissions scenarios than for the high-emissions scenarios in the ensemble members provided to the CMIP6 archive (Table S4). For all scenarios, the first year of practically sea ice-free conditions ranges from some years before present to the end of this century (Table S4), with a clear majority of models reaching ice-free conditions before 2050. This finding remains valid for the selected models. From the middle of the century onward, scenario dependence becomes more and more evident. For example, the loss of sea-ice area in March occurs much faster from 2050 onward in scenario SSP5-8.5 than in other scenarios (Figure 2c).

5. Conclusion

Based on the analyzed evolution of Arctic sea-ice area and volume in CMIP6 models, in this contribution we have found the following:

- CMIP6 model performance in simulating Arctic sea ice is similar to CMIP3 and CMIP5 model performance in many aspects. This includes models simulating a wide spread of mean sea-ice area and volume in March and September; the multimodel ensemble spread capturing the observed mean sea-ice area in March and September; the models' general underestimation of the sensitivity of September sea-ice area to a given amount of global warming; and most models' failure to simulate at the same time a plausible evolution of sea-ice area and of GMST.
- CMIP6 model performance differs from CMIP3 and CMIP5 in some aspects. These include a larger fraction of CMIP6 models capturing the observed sensitivity of Arctic sea ice to anthropogenic CO_2 emissions and the CMIP6 multimodel ensemble mean being closer to the observed sensitivity of Arctic sea ice to global warming. It is unclear to what degree these improvements are caused by a change in the forcing versus improvement of model physics.
- The CMIP6 models simulate a large spread for when Arctic sea-ice area is predicted to drop below 1×10^6 km^2, such that the Arctic Ocean becomes practically sea-ice free. However, the clear majority of all models, and of those models that best capture the observed evolution, project that the Arctic will become practically sea ice free in September before the year 2050 at future anthropogenic CO_2 emissions of less than 1000 $GtCO_2$ above that of 2019 in all scenarios.

Appendix A: Authors and Affiliations

All authors contributed to discussions and the writing of the paper, as well as implementation or analysis of SIMIP variables in CMIP6 models. Additional contributions are listed below.

Dirk Notz, Center for Earth System Research and Sustainability (CEN), University of Hamburg and Max Planck Institute for Meteorology, Hamburg, Germany, cochair of SIMIP, led the development of this paper, contributed to implementing the SIMIP protocol in MPI-ESM

Jakob Dörr, Max Planck Institute for Meteorology, Hamburg, Germany, carried out all data analysis for this paper and compiled all figures and tables

David A. Bailey, Climate and Global Dynamics Laboratory, National Center for Atmospheric Research, Boulder, CO, USA

Ed Blockley, Met Office Hadley Centre, Exeter, UK, contributed to the sea ice component of the UKESM and HadGEM3 models

Mitchell Bushuk, Geophysical Fluid Dynamics Laboratory, Princeton, NJ, USA

Jens Boldingh Debernard, Norwegian Meteorological Institute, Oslo, Norway, contributed to the sea ice component of NorESM2-LM

Evelien Dekker, Rossby Centre, Swedish Meteorological and Hydrological Institute, Norrköping, Meteorological Department at Stockholm University, Stockholm, Sweden

Patricia DeRepentigny, Department of Atmospheric and Oceanic Sciences and Institute of Arctic and Alpine Research, University of Colorado Boulder, Boulder, CO, USA

David Docquier, Rossby Centre, Swedish Meteorological and Hydrological Institute, Norrköping, Sweden

Neven S. Fučkar, Environmental Change Institute, University of Oxford, Oxford, UK, and Earth Sciences Department, Barcelona Supercomputing Center, Barcelona, Spain

John C. Fyfe, Canadian Centre for Climate Modelling and Analysis, Environment and Climate Change Canada, Ottawa, Ontario, Canada

Alexandra Jahn, Department of Atmospheric and Oceanic Sciences and Institute of Arctic and Alpine Research, University of Colorado Boulder, Boulder, CO, USA; cochair of SIMIP

Marika Holland, Climate and Global Dynamics Laboratory, National Center for Atmospheric Research, Boulder, CO, USA; SIMIP steering-group member

Elizabeth Hunke, Theoretical Division, Los Alamos National Laboratory, Los Alamos, NM, USA; SIMIP steering-group member

Doroteaciro Iovino, Ocean Modeling and Data Assimilation Division, Centro Euro-Mediterraneo sui Cambiamenti Climatici, Lecce, Italy

Narges Khosravi, Alfred Wegener Institute, Helmholtz Centre for Polar and Marine Research, Bremerhaven, Germany

Gurvan Madec, Sorbonne Université, UPMC Paris 6, LOCEAN-IPSL, CNRS/IRD/MNHN, Paris, France

François Massonnet, Georges Lematre Centre for Earth and Climate Research, Earth and Life Institute, Université catholique de Louvain, Louvain-la-Neuve, Belgium; SIMIP steering-group member

Siobhan O'Farrell, CSIRO Oceans and Atmosphere, Aspendale, Victoria, Australia

Alek Petty, Cryospheric Sciences Laboratory, NASA Goddard Space Flight Center, Greenbelt, Maryland, United States of America, and Earth System Science Interdisciplinary Center, University of Maryland, College Park, MD, USA

Arun Rana, Georges Lematre Centre for Earth and Climate Research, Earth and Life Institute, Université Catholique de Louvain, Louvain-la-Neuve, Belgium

Lettie Roach, Atmospheric Sciences, University of Washington, Seattle, WA, United States of America

Erica Rosenblum, Centre for Earth Observation Science, University of Manitoba, Winnipeg, Manitoba, Canada; contributed to the preliminary data analysis

Clement Rousset, Sorbonne Universitié, UPMC Paris 6, LOCEAN-IPSL, CNRS/IRD/MNHN, Paris, France

Tido Semmler, Alfred Wegener Institute, Helmholtz Centre for Polar and Marine Research, Bremerhaven, Germany

Julienne Stroeve, University College London, London, UK, and National Snow and Ice Data Center, Boulder, CO, USA; SIMIP steering-group member

Takahiro Toyoda, Meteorological Research Institute, Japan Meteorological Agency, Japan; contributed to carry out the MRI-ESM2 experiments and to prepare the output for SIMIP analyses

Bruno Tremblay, Department of Atmospheric and Oceanic Sciences, McGill University, Montreal, Canada; SIMIP steering-group member

Hiroyuki Tsujino, Meteorological Research Institute, Japan Meteorological Agency, Japan; contributed to carry out the MRI-ESM2 experiments and to prepare the output for SIMIP analyses

Acknowledgments
We thank two anonymous reviewers for their valuable feedback that helped improving this manuscript. We are grateful to all modeling centers for carrying out CMIP6 simulations used here. The data used for this study are freely available from the Earth System Grid Federation (ESGF) (esgf-node.llnl.gov/search/cmip6). See supporting information for a detailed listing of all CMIP6 data sets used in this study, including their dois. The scripts for analysis and plotting of the data are available from the GitHub (https://github.com/jakobdoerr/SIMIP_2020). EC-Eart3-Veg simulations that are not published on ESGF yet are locally stored at the Swedish Meteorological and Hydrological Institute (cmip6-data@ecearth.org). We thank the EC-Earth consortium that realized the development of EC-Earth. The EC-Earth3-Veg simulations were done as part of the European Union's Horizon 2020 research and innovation programme under Grant Agreement No 641816 (CRESCENDO) on resources provided by the Swedish National Infrastructure for Computing (SNIC) at PDC and NSC. Previous and current CESM versions are freely available online (www.cesm.ucar.edu/models). The CESM project is supported primarily by the National Science Foundation (NSF). This material is based upon work supported by the National Center for Atmospheric Research, which is a major facility sponsored by the NSF under Cooperative Agreement 1852977. Computing and data storage resources, including the Cheyenne supercomputer (doi:10.5065/D6RX99HX), were provided by the Computational and Information Systems Laboratory (CISL) at NCAR. We thank all the scientists, software engineers, and administrators who contributed to the development of CESM2. The ACCESS-CM2 CMIP6 submission was jointly funded through CSIRO and the Earth Systems and Climate Change Hub of the Australian Government's National Environmental Science Program, with support from the Australian Research Council Centre of Excellence for Climate System Science. The ACCESS-ESM1.5 CMIP6 submission was supported by the CSIRO Climate Science Centre. Parts of the work described in this paper has received funding from the European Union's Horizon 2020 Research and Innovation programme through Grant Agreement 727862 APPLICATE. The content of the paper is the sole responsibility of the authors, and it does not represent the opinion of the European Commission, and the Commission is not responsible for any use that might be made of information

Martin Vancoppenolle, Sorbonne Universitié, UPMC Paris 6, LOCEAN-IPSL, CNRS/IRD/MNHN, Paris, France; SIMIP steering-group member; contributed to the sea ice component of IPSL-CM and EC-Earth

References

Bunzel, F., Notz, D., & Pedersen, L. T. (2018). Retrievals of Arctic sea-ice volume and its trend significantly affected by interannual snow variability. *Geophysical Research Letters*, *45*, 11,751–11,759. https://doi.org/10.1029/2018GL078867

Cavalieri, D. J., Parkinson, C. L., Gloersen, P., & Zwally, H. J. (1997). Arctic and Antarctic sea ice concentrations from multichannel passive-microwave satellite data sets: October 1978 to December 1996 (Technical Memorandum 104647): NASA.

Checa-Garcia, R., Hegglin, M. I., Kinnison, D., Plummer, D. A., & Shine, K. P. (2018). Historical tropospheric and stratospheric ozone radiative forcing using the CMIP6 database. *Geophysical Research Letters*, *45*, 3264–3273. https://doi.org/10.1002/2017GL076770

Chevallier, M., Smith, G. C., Dupont, F., Lemieux, J. F., Forget, G., Fujii, Y., & Wang, X. (2017). Intercomparison of the Arctic sea ice cover in global ocean-sea ice reanalyses from the ORA-IP project. *Climate Dynamics*, *49*(3), 1107–1136. https://doi.org/10.1007/s00382-016-2985-y

Comiso, J. C., Cavalieri, D. J., Parkinson, C. L., & Gloersen, P. (1997). Passive microwave algorithms for sea ice concentration: A comparison of two techniques. *Remote Sensing of Environment*, *60*(3), 357–384. https://doi.org/10.1016/S0034-4257(96)00220-9

Comiso, J. C., Meier, W. N., & Gersten, R. (2017). Variability and trends in the Arctic sea ice cover: Results from different techniques. *Journal of Geophysical Research: Oceans*, *122*, 6883–6900. https://doi.org/10.1002/2017JC012768

England, M., Jahn, A., & Polvani, L. (2019). Nonuniform contribution of internal variability to recent arctic sea ice loss. *Journal of Climate*, *32*(13), 4039–4053. https://doi.org/10.1175/JCLI-D-18-0864.1

Eyring, V., Bony, S., Meehl, G. A., Senior, C., Stevens, B., Stouffer, R. J., & Taylor, K. E. (2015). Overview of the Coupled Model Intercomparison Project Phase 6 (CMIP6) experimental design and organisation. *Geoscientific Model Development*, *8*(12), 10,539–10,583. https://doi.org/10.5194/gmdd-8-10539-2015

GISTEMP Team (2019). GISS Surface Temperature Analysis (GISTEMP), version 4. Goddard Institute for Space Studies [date accessed: XX/XX/XX]. Retrieved from https://data.giss.nasa.gov/gistemp/

Gidden, M., Riahi, K., Smith, S., Fujimori, S., Luderer, G., Kriegler, E., et al. (2019). Global emissions pathways under different socioeconomic scenarios for use in CMIP6: A dataset of harmonized emissions trajectories through the end of the century. *Geoscientific model development*, *12*(4), 1443–1475. https://doi.org/10.5194/gmd-12-1443-2019

Global Carbon Project (2019). Supplemental data of Global Carbon Budget 2019 (Version 1.0 [Data set]. https://doi.org/10.18160/gcp-2019

Gregory, J. M., Stott, P. A., Cresswell, D. J., Rayner, N. A., Gordon, C., & Sexton, D. M. H. (2002). Recent and future changes in Arctic sea ice simulated by the HadCM3 AOGCM. *Geophysical Research Letters*, *29*(24), 2175. https://doi.org/10.1029/2001GL014575

Herrington, T., & Zickfeld, K. (2014). Path independence of climate and carbon cycle response over a broad range of cumulative carbon emissions. *Earth System Dynamics*, *5*, 409–422. https://doi.org/10.5194/esd-5-409-2014

Jahn, A. (2018). Reduced probability of ice-free summers for 1.5°C compared to 2°C warming. *Nature Climate Change*, *8*, 409-413. https://doi.org/10.1038/s41558-018-0127-8

Jahn, A., Kay, J. E., Holland, M. M., & Hall, D. M. (2016). How predictable is the timing of a summer ice-free Arctic? *Geophysical Research Letters*, *43*, 9113–9120. https://doi.org/10.1002/2016GL070067

Kay, J. E., Holland, M. M., & Jahn, A. (2011). Inter-annual to multi-decadal Arctic sea ice extent trends in a warming world. *Geophysical Research Letters*, *38*, L15708. https://doi.org/10.1029/2011GL048008

Koenigk, T., Devasthale, A., & Karlsson, K. G. (2014). Summer Arctic sea ice albedo in CMIP5 models. *Atmospheric Chemistry and Physics*, *14*(4), 1987–1998. https://doi.org/10.5194/acp-14-1987-2014

Lavergne, T., Sørensen, A. M., Kern, S., Tonboe, R., Notz, D., Aaboe, S., & Pedersen, L. T. (2019). Version 2 of the EUMETSAT OSI SAF and ESA CCI sea-ice concentration climate data records. *The Cryosphere*, *13*(1), 49–78. https://doi.org/10.5194/tc-13-49-2019

Lenssen, N. J., Schmidt, G. A., Hansen, J. E., Menne, M. J., Persin, A., Ruedy, R., & Zyss, D. (2019). Improvements in the GISTEMP uncertainty model. *Journal of Geophysical Research: Atmospheres*, *124*, 6307–6326. https://doi.org/10.1029/2018JD029522

Mahlstein, I., & Knutti, R. (2012). September Arctic sea ice predicted to disappear near 2°C global warming above present. *Journal of Geophysical Research*, *117*, D06104. https://doi.org/10.1029/2011JD016709

Massonnet, F., Fichefet, T., Goosse, H., Bitz, C. M., Philippon-Berthier, G., Holland, M. M., & Barriat, P. Y. (2012). Constraining projections of summer Arctic sea ice. *The Cryosphere*, *6*(6), 1383–1394. https://doi.org/10.5194/tc-6-1383-2012

Melia, N., Haines, K., & Hawkins, E. (2015). Improved Arctic sea ice thickness projections using bias-corrected CMIP5 simulations. *The Cryosphere*, *9*(6), 2237–2251. https://doi.org/10.5194/tc-9-2237-2015

Morice, C. P., Kennedy, J. J., Rayner, N. A., & Jones, P. D. (2012). Quantifying uncertainties in global and regional temperature change using an ensemble of observational estimates: The HadCRUT4 data set. *Journal of Geophysical Research*, *117*, D08101. https://doi.org/10.1029/2011JD017187

Niederdrenk, A. L., & Notz, D. (2018). Arctic sea ice in a 1.5°C warmer world. *Geophysical Research Letters*, *45*(4), 1963–1971. https://doi.org/10.1002/2017GL076159

Notz, D. (2014). Sea-ice extent and its trend provide limited metrics of model performance. *The Cryosphere*, *8*(1), 229–243. https://doi.org/10.5194/tc-8-229-2014

Notz, D. (2015). How well must climate models agree with observations? *Philosophical Transactions of the Royal Society A*, *373*(2052), 20140164. https://doi.org/10.1098/rsta.2014.0164

Notz, D., Jahn, A., Holland, M., Hunke, E., Massonnet, F., Stroeve, J., & Vancoppenolle, M. (2016). Sea Ice Model Intercomparison Project (SIMIP): Understanding sea ice through climate-model simulations. *Geoscientific Model Development Discussions*, *9*, 3427–3446. https://doi.org/10.5194/gmd-2016-67

Notz, D., & Stroeve, J. (2016). Observed Arctic sea-ice loss directly follows anthropogenic CO_2 emission. *Science*, *354*, 747–750. https://doi.org/10.1126/science.aag2345

Notz, D., & Stroeve, J. (2018). The trajectory towards a seasonally ice-free Arctic Ocean. *Current Climate Change Reports*, *4*(4), 407–416. https://doi.org/10.1007/s40641-018-0113-2

O'Neill, B. C., Tebaldi, C., Van Vuuren, D. P., Eyring, V., Friedlingstein, P., Hurtt, G., & Sanderson, B. M. (2016). The Scenario Model Intercomparison Project (ScenarioMIP) for CMIP6. *Geoscientific Model Development*, *9*(9), 3461–3482. https://doi.org/10.5194/gmd-9-3461-2016

Olason, E., & Notz, D. (2014). Drivers of variability in Arctic sea-ice drift speed. *Journal of Geophysical Research: Oceans*, *119*, 5755–5775. https://doi.org/10.1002/2014JC009897

contained. We thank the WCRP-CliC Project for supporting the SIMIP project. E. Blockley was supported by the Joint UK BEIS/Defra Met Office Hadley Centre Climate Programme (GA01101). J. B. Debernard is supported by the Research Concile of Norway through INES (270061). E. Dekker is supported by the Arctic Across Scales Project through the Knut and Alice Wallenberg Foundation (KAW2016.0024). P. DeRepentigny is supported by the Natural Sciences and Engineering Council of Canada, the Fond de recherche du Qubec-Nature et Technologies, and the Canadian Meteorological and Oceanographic Society through PhD scholarships and NSF-OPP Award 1847398. D. Docquier is funded by the EU Horizon 2020 OSeaIce project, under the Marie Sklodowska-Curie Grant Agreement 834493. J. Dörr is funded by the German Ministry for Education and Research through the project "Meereis bei +1.5°C." N. S. Fučkar acknowledges support of H2020 MSCA IF (Grant ID 846824). E. Hunke is supported by the Regional and Global Modeling and Analysis program of the Department of Energy's Biological and Environmental Research division. A. Jahn's contribution is supported by NSF-OPP Award 1847398. F. Massonnet is a F.R.S.-FNRS Research Fellow. D. Notz is funded by the Deutsche Forschungsgemeinschaft under Germanys Excellence Strategy EXC 2037 'CLICCS - Climate, Climatic Change, and Society' Project Number: 390683824, contribution to the Center for Earth System Research and Sustainability (CEN) of Universität Hamburg. L. Roach was supported by the National Science Foundation Grant PLR-1643431 and National Oceanic and Atmospheric Administration Grant NA18OAR4310274. J. Stroeve and E. Rosenblum are supported by the Canada C150 Chair Program. This work is a contribution to NSF-OPP Award 1504023 awarded to B. Tremblay.

Olonscheck, D., & Notz, D. (2017). Consistently estimating internal climate variability from climate model simulations. *Journal of Climate*, *30*(23), 9555–9573. https://doi.org/10.1175/JCLI-D-16-0428.1

Riahi, K., van Vuuren, D. P., Kriegler, E., Edmonds, J., O'Neill, B. C., Fujimori, S., & Tavoni, M. (2017). The Shared Socioeconomic Pathways and their energy, land use, and greenhouse gas emissions implications: An overview. *Global Environmental Change*, *42*, 153–168. https://doi.org/10.1016/j.gloenvcha.2016.05.009

Ridley, J., & Blockley, E. (2018). Solar radiation management not as effective as CO_2 mitigation for Arctic sea ice loss in hitting the 1.5 and 2°C COP climate targets. *The Cryosphere*, *12*, 3355–3360. https://doi.org/10.5194/tc-12-3355-2018

Roach, L. A., Dörr, J., Holmes, C. R., Massonnet, F., Blockley, E. W., Notz, D., & Bitz, C. M. (2020). Antarctic sea ice in CMIP6. *Geophysical Research Letters*, *47*, e2019GL086729. https://doi.org/10.1029/2019GL086729

Rohde, R., Muller, R., Jacobsen, R., Perlmutter, S., & Mosher, S. (2013). Berkeley Earth temperature averaging process. *Geoinformatics & Geostatistics: An Overview*, *1*, 2. https://doi.org/10.4172/2327-4581.1000103

Rosenblum, E., & Eisenman, I. (2016). Faster Arctic sea ice retreat in CMIP5 than in CMIP3 due to volcanoes. *Journal of Climate*, *29*(24), 9179–9188. https://doi.org/10.1175/JCLI-D-16-0391.1

Rosenblum, E., & Eisenman, I. (2017). Sea ice trends in climate models only accurate in runs with biased global warming. *Journal of Climate*, *30*(16), 6265–6278. https://doi.org/10.1175/JCLI-D-16-0455.1

Screen, J. A., & Williamson, D. (2017). Ice-free Arctic at 1.5°C? *Nature Climate Change*, *7*(4), 230–231. https://doi.org/10.1038/nclimate3248

Shu, Q., Song, Z., & Qiao, F. (2015). Assessment of sea ice simulations in the CMIP5 models. *The Cryosphere*, *9*(1), 399–409. https://doi.org/10.5194/tc-9-399-2015

Sigmond, M., Fyfe, J. C., & Swart, N. C. (2018). Ice-free Arctic projections under the Paris Agreement. *Nature Climate Change*, *8*, 404–408. https://doi.org/10.1038/s41558-018-0124-y

Stroeve, J., Barrett, A., Serreze, M., & Schweiger, A. (2014). Using records from submarine, aircraft and satellites to evaluate climate model simulations of Arctic sea ice thickness. *The Cryosphere*, *8*(5), 1839–1854. https://doi.org/10.5194/tc-8-1839-2014

Stroeve, J., Holland, M. M., Meier, W., Scambos, T., & Serreze, M. (2007). Arctic sea ice decline: Faster than forecast. *Geophysical Research Letters*, *34*, L09501. https://doi.org/10.1029/2007GL029703

Stroeve, J., Kattsov, V., Barrett, A., Serreze, M., Pavlova, T., Holland, M., & Meier, W. N. (2012). Trends in Arctic sea ice extent from CMIP5, CMIP3 and observations. *Geophysical Research Letters*, *39*, L16502. https://doi.org/10.1029/2012GL052676

Stroeve, J., & Notz, D. (2015). Insights on past and future sea-ice evolution from combining observations and models. *Global and Planetary Change*, *135*, 119–132. https://doi.org/10.1016/j.gloplacha.2015.10.011

Swart, N. C., Fyfe, J. C., Hawkins, E., Kay, J. E., & Jahn, A. (2015). Influence of internal variability on Arctic sea-ice trends. *Nature Climate Change*, *5*(2), 86–89. https://doi.org/10.1038/nclimate2483

Vose, R. S., Arndt, D., Banzon, V. F., Easterling, D. R., Gleason, B., Huang, B., & Wuertz, D. B. (2012). NOAA's merged land-ocean surface temperature analysis. *Bulletin of the American Meteorological Society*, *93*(11), 1677–1685. https://doi.org/10.1175/BAMS-D-11-00241.1

Winton, M. (2011). Do climate models underestimate the sensitivity of Northern Hemisphere sea ice cover? *Journal of Climate*, *24*(15), 3924–3934.

Zelinka, M. D., Myers, T. A., McCoy, D. T., Po-Chedley, S., Caldwell, P. M., Ceppi, P., & Taylor, K. E. (2020). Causes of higher climate sensitivity in CMIP6 models. *Geophysical Research Letters*, *47*, e2019GL085782. https://doi.org/10.1029/2019GL085782

Zickfeld, K., Arora, V. K., & Gillett, N. P. (2012). Is the climate response to CO_2 emissions path dependent? *Geophysical Research Letters*, *39*, L05703. https://doi.org/10.1029/2011GL050205

Zygmuntowska, M., Rampal, P., Ivanova, N., & Smedsrud, L. H. (2014). Uncertainties in Arctic sea ice thickness and volume: New estimates and implications for trends. *The Cryosphere*, *8*(2), 705–720. https://doi.org/10.5194/tc-8-705-2014